Available online at www.sciencedirect.com

Resuscitation

journal homepage: www.elsevier.com/locate/resuscitation

Clinical paper

Postmortem histopathology of electroencephalography and evoked potentials in postanoxic coma

Michel J.A.M. van Putten[a,b,*], *Casper Jansen*[c], *Marleen C. Tjepkema-Cloostermans*[a], *Tim M.J. Beernink*[a], *Rob Koot*[g], *Frank Bosch*[f], *Albertus Beishuizen*[e], *Jeannette Hofmeijer*[d,b]

[a] *Clinical Neurophysiology, Medisch Spectrum Twente, Enschede, The Netherlands*
[b] *Clinical Neurophysiology, University of Twente, PO Box 217, 7500 KA Enschede, The Netherlands*
[c] *Laboratorium Pathologie Oost-Nederland, Hengelo, The Netherlands*
[d] *Rijnstate Ziekenhuis, Arnhem, Nijmegen, The Netherlands*
[e] *Department of Intensive Care Medicine, Medisch Spectrum Twente, Enschede, The Netherlands*
[f] *Department of Pathology, Rijnstate Ziekenhuis, Arnhem, The Netherlands*
[g] *Department of Intensive Care Medicine, Rijnstate Ziekenhuis, Arnhem, The Netherlands*

Abstract

Early EEG patterns and SSEP responses are associated with neurological recovery of comatose patients with postanoxic encephalopathy after cardiac arrest. However, the nature and distribution of brain damage underlying the characteristic EEG and SSEP patterns are unknown. We relate EEG and SSEP findings with results from histological analyses of the brains of eleven non-survivors. With restoration towards continuous rhythms within 24 h after cardiac arrest, no signs of structural neuronal damage were observed. Absent SSEP responses were always accompanied by thalamic damage. Pathological burst suppression patterns were associated with a variable degree of neuronal damage to cortex, cerebellum and hippocampus. In patients with additional thalamic involvement, burst-suppression with identical bursts was observed, a characteristic EEG pattern presumably reflecting residual activity from a relatively isolated and severely compromised cortex.

Keywords: Postanoxic coma, EEG, SSEP, Postmortem histopathology, Prognostication

Introduction

Electroencephalographic (EEG) and somatosensory evoked potential (SSEP) recordings in patients with postanoxic encephalopathy following cardiac arrest hold valuable information for prediction of neurological outcome. An evolution towards continuous EEG rhythms within 12 h after cardiac arrest is strongly related to a full neurological recovery.[7,15,31,42,35] In contrast, persistent iso-electricity or low voltage EEG, burst-suppression with identical bursts, or absent evoked cortical responses, are strongly associated with a poor neurological outcome.[17,15,7,31,42,35] EEG rhythms primarily reflect the summation of postsynaptic currents of pyramidal cells, but it is largely unknown which patterns of brain damage correlate with particular pathological EEG rhythms in postanoxic coma. Since EEG and SSEP are complementary for detection of patients with a poor outcome,[15] pathological EEG and SSEP recordings probably reflect different

* Corresponding author.
E-mail address: m.j.a.m.vanputten@utwente.nl (M.J.A.M. van Putten).
https://doi.org/10.1016/j.resuscitation.2018.12.007
Received 4 October 2018; Received in revised form 17 November 2018; Accepted 10 December 2018

patterns of irreversible brain damage.[32,39] However, the relation between these EEG patterns and the nature and extent of neuronal damage is largely unknown.

Synaptic arrest is an early consequence of ischaemia and occurs within seconds of moderately reduced perfusion levels (10–35 ml/100 g/min).[40] Early synaptic failure results from presynaptic damage with impaired transmitter release.[18,10,2] While short-term synaptic depression probably affects both excitatory and inhibitory synapses,[24] excitatory neurotransmission can be increased in severe cases,[27,38,23] which may result in electrographic seizures.[32] Without timely recovery of cerebral perfusion, disturbances of synaptic transmission may become permanent, even with preserved membrane potentials.[2,16] Synaptic damage goes along with pathological EEG patterns or somatosensory evoked potentials,[15] but cannot be visualized with conventional imaging techniques.[2,25]

Lower perfusion levels, around 5–10 ml/100 g/min, lead to malfunctioning of energy dependent ion pumps, especially the ATP dependent sodium–potassium pumps in the neuronal and glial plasma membranes.[1] This causes loss of ion gradients across the cell membrane (depolarization) and inability to generate action potentials. With failure of transmembrane sodium–potassium pumps, the net inflow of osmotically active particles (sodium, chloride) is larger than the outflow (potassium), causing an increased intracellular osmolality, with an inflow of water, and swelling of neuronal and glial cells.[33,9] Only then, damage can be visualized with for example diffusion weighted imaging.[25]

Neurons have a differential sensitivity to ischemia. For instance, while pyramidal neurons of the cortex can quickly depolarize after ischemia, magnocellular neuroendocrine cells under identical stress resist complete depolarization.[3] Selective neuronal damage has also been denoted with regard to spatial variations, gray matter being more vulnerable than white matter, and hippocampus, cerebellar Purkinje cells, pyramidal cells in the neocortex, and parts of thalamus and striatum more than other cortical areas.[28,5,29] In an experimental focal ischemic stroke in mice, cortical layers II/III and deep V were most susceptible to the effects of ischemia, with more pronounced reductions of neurons, astrocytes and microglia than in other cortical layers, and cellular changes were most prominent in layer V.[8]

In this study, for the first time, we associate EEG and SSEP patterns with the spatial distribution of hypoxic–ischemic brain damage by postmortem histological analyses of brains from non-surviving patients with a postanoxic encephalopathy after cardiac arrest.

Materials and methods

This study is embedded in a prospective cohort study in two Hospitals (MST and Rijnstate) on EEG monitoring in coma after cardiac arrest between 2011 and 2016. Details are described elsewhere.[15] Of all patients that died in the hospital, permission to perform autopsy had been requested. The Medical Ethical Committee Twente approved the protocol and waived the need for informed consent for EEG monitoring. Permission for autopsy was obtained from legal representatives.

Patients and treatment

Consecutive, adult, comatose patients after cardiac arrest (Glasgow Coma Scale score $\leq$8), admitted to the ICU, were included in our cohort study. Patients were treated according to standard protocols for comatose patients after cardiac arrest. Targeted temperature management included mild therapeutic hypothermia (33–36 °C) induced as soon as possible after arrival at the emergency room or ICU and maintained for 24 h. After 24 h, passive rewarming was controlled to a speed of 0.25–0.5 °C per hour. Propofol or midazolam and fentanyl were used for sedation. Analgosedation was usually discontinued at a body temperature of 36.5 °C. Decisions on withdrawal of treatment were based on international guidelines including evaluation of brainstem reflexes, non-responding myoclonus to treatment, and bilateral absence of evoked somatosensory evoked potentials (SSEPs). EEG patterns within the first three days were not taken into account.

EEG and SSEP recordings

Continuous EEG started as soon as possible after arrival at the ICU and continued for at least 3 days, or until time of death. EEGs were recorded using twenty-one silver/silver chloride cup electrodes were placed on the scalp according to the international 10–20 system. Somatosensory evoked potentials (SSEPs) were recorded after electrical stimulation of the right and left median nerve using a bipolar surface electrode at the wrist. Stimulus duration was 0.3 ms, and stimulus amplitude was adjusted until a visible twitch was produced. Two sets of >200 responses were averaged, band pass filtered between 0.1 Hz and 2.5 kHz, and notch filtered around 50 Hz. Stimulus frequency was set at 1.7 Hz. Silver–silver-chloride cup electrodes were placed at the elbow, Erb's point, cervical spine (C5), and 2 cm posterior to C3 and C4 (C3′ and C4′). Fz was used as a reference electrode. SSEP recordings were made using a Nicolet Bravo system (Viasys, Houten, The Netherlands).

EEG classification

EEG analyses were performed off-line, after the registrations. The EEG was classified as iso-electric, low-voltage (<20 μV), epileptiform (including evolving electrographic seizures and generalized periodic discharges (GPDs)), burst-suppression with or without identical bursts, or continuous patterns >20 μV with frequencies <4 Hz, 4–8 Hz or ≥8 Hz.[7,15]

Postmortem analysis

Brains were removed at autopsy and fixed in 10% phosphate-buffered formalin for at least six weeks, prior to sectioning. After macroscopic evaluation, histopathological examination was performed on 5 μm-thick sections of formalin-fixed and paraffin-embedded brain tissue blocks. Sections were taken from the following areas: frontal (superior and middle frontal gyri), parietal (superior and middle parietal gyri), temporal (middle temporal gyrus) and occipital (calcarine cortex) cortices, hippocampus (Ammon's horn) with trans(entorhinal) cortex, striatum (caudate nucleus, putamen and globus pallidus), thalamus, amygdala, cingulate gyrus, brainstem (midbrain including periaqueductal gray, pons including locus coeruleus, and medulla oblongata including inferior olive nucleus) and cerebellum. Haematoxylin–eosin stains were performed according to standard procedures.

Acute and sub-acute lesions were characterized by the presence of neurons with shrunken pyknotic nuclei and brightly eosinophilic cytoplasm. In addition, vacuolization of the neuropil may be seen.

Ischemic damage was scored semi-quantitatively by counting the number of red neurons per high power field in a brain region of interest.

Scores were defined as mild (+, <5% of neurons affected), moderate (++, 5–50% of neurons affected) and severe (+++, >50% of neurons affected).

Association of EEG and histopathology

Associations between EEG patterns and postmortem findings are presented in a descriptive way, and analyzed qualitatively.

Results

Eleven patients were included. EEG recordings started within 15 h after cardiac arrest. Baseline characteristics are summarized in Table 1. Two patients had early (<24 h) myoclonic status (cases 1, 9). In all patients, brain stem reflexes were preserved. Nine patients died after withdrawal of life sustaining treatment based on a predicted poor neurological outcome. Two patients (cases 3 and 10) initially had good neurological recovery, but died immediately after a second cardiac arrest in the intensive care unit. These patients had continuous EEG patterns within 24 h after the first cardiac arrest. In all other patients, EEG patterns within 24 h after cardiac arrest were pathological with burst-suppression patterns with flat (<10 μV) interburst intervals. Five patients showed burst suppression with identical bursts (cases 2, 5, 7, 8, 11); in one patient bursts evolved to generalized periodic discharges (case 9), or bursts with spikes and spike waves (case 1). Bursts in cases 4 and 6 were heterogeneous, with very long interburst intervals of 10–15 min (case 4) or low voltage bursts (10–25 μV; case 6). Examples of characteristic EEGs patterns are shown in Fig. 1.

Ten autopsies were performed within 24 h after death, one after 60 h. Average brain weight was 1438 g and correlated with age ($R = 0.86$, $p = 0.0006$). Macroscopic evaluation of the brain showed no cortical abnormalities in any of the patients. In several patients, the basal ganglia showed ischaemic hemorrhagic transformation, most prominent in case 2. Microscopic evaluation showed no areas of hypoxic–ischemic damage in the two patients (cases 3 and 10) with intrinsic good neurological recovery. In all other patients, morphological changes of hypoxic brain injury was present, characterized by cellular degeneration with shrinkage, the presence of neurons with shrunken nuclei, brightly eosinophilic cytoplasm ('red neurons'), and loss of Nissl substance in variable brain regions. Four patients had hypoxic–ischemic damage of the deep layers of the cerebral cortex, cerebellar Purkinje cells and/or hippocampus. Three patients had additional histological signs of hypoxic–ischemic damage in the deep subcortical brain structures, including the basal ganglia. The mesencephalon was affected in a single patient (case 2) and the pons in three patients (cases 2, 5, 8). In both patients with a myoclonic status, Purkinje cells in the cerebellum were affected with mild cortical and absent (case 9) or mild (case 1) thalamic involvement. Examples of histological findings are presented in Fig. 2.

EEG and SSEP in relation to histopathology

Identical bursts were only present in all five patients (2, 5, 7, 8, 11) with both severe (>50%) thalamic, cerebellar and moderate (5–50%, patient 5) to severe (>50%, patients 2, 7, 8, 11) cortical involvement. In patients with other burst suppression patterns, mainly the cortex and cerebellum were affected, while deeper brain structures were relatively preserved, in particular the thalamus showed no or only limited hypoxic damage. A continuous EEG within 24 h after arrest was associated with absence of structural hypoxic–ischemic brain damage. The two patients with mild to moderate hypoxic ischemic damage to the cortex, but without thalamic involvement, had a preserved SSEP (cases 4 and 9). In the two patients with minor thalamic damage (cases 3, 6), in one the SSEP was absent (case 3). In all patients with moderate to severe damage to the thalamus, the cortical evoked potential was absent. Results of histological examination in relation to EEG and SSEP are summarized in Table 2.

Discussion

For the first time, we relate early EEG and SSEP patterns in comatose patients with postanoxic encephalopathy after cardiac arrest to the distribution of hypoxic–ischemic brain damage derived from postmortem histological analyses. We chose to correlate postmortem findings with EEG patterns observed in the first 24 h after arrest as these patterns are most distinct and correlate best with neurological outcome.[15,35] We show that burst suppression with identical bursts, a prognostically invariably poor EEG pattern,[15] is associated with the most severe widespread damage, including cerebral cortex, cerebellum, hippocampus and thalamus. This EEG pattern presumably reflects residual activity of a relatively isolated and severely compromised cortex. All patients with such burst-suppression patterns have a poor prognosis, most die, and those who survive have severe neurological deficits.[35] In patients with other burst suppression patterns, brain damage was limited to the cortex and

Table 1 – Baseline characteristics. t.o.d.: time of death after arrest. t.o.a.: time of autopsy after death.

Case	Age	Sex	Setting	Cause	Initial rhythm	t.o.d.	t.o.a. (h)
1	77	m	OHCA	Unknown	Unknown	1 d 20 h	13
2	72	m	OHCA	Cardiac	Unknown	1 d 22 h	16
3	51	m	OHCA	Cardiac	Unknown	2 d 12 h	12
4	59	m	OHCA	Cardiac	Asystole	5 d 4 h	12
5	55	m	OHCA	Unknown	Asystole	1 d 18 h	62
6	61	m	IHCA	Asphyxia	VF	4 d 8 h	17
7	67	m	IHCA	Cardiac	PEA	3 d 16 h	18
8	78	m	OHCA	Cardiac	VF	3 d 5 h	12
9	63	m	OHCA	Cardiac	VF	6 d 18 h	<24
10	72	f	OHCA	Cardiac	VF	2 d 12 h	<24
11	61	m	OHCA	Unknown	Asystole	3 d 18 h	7

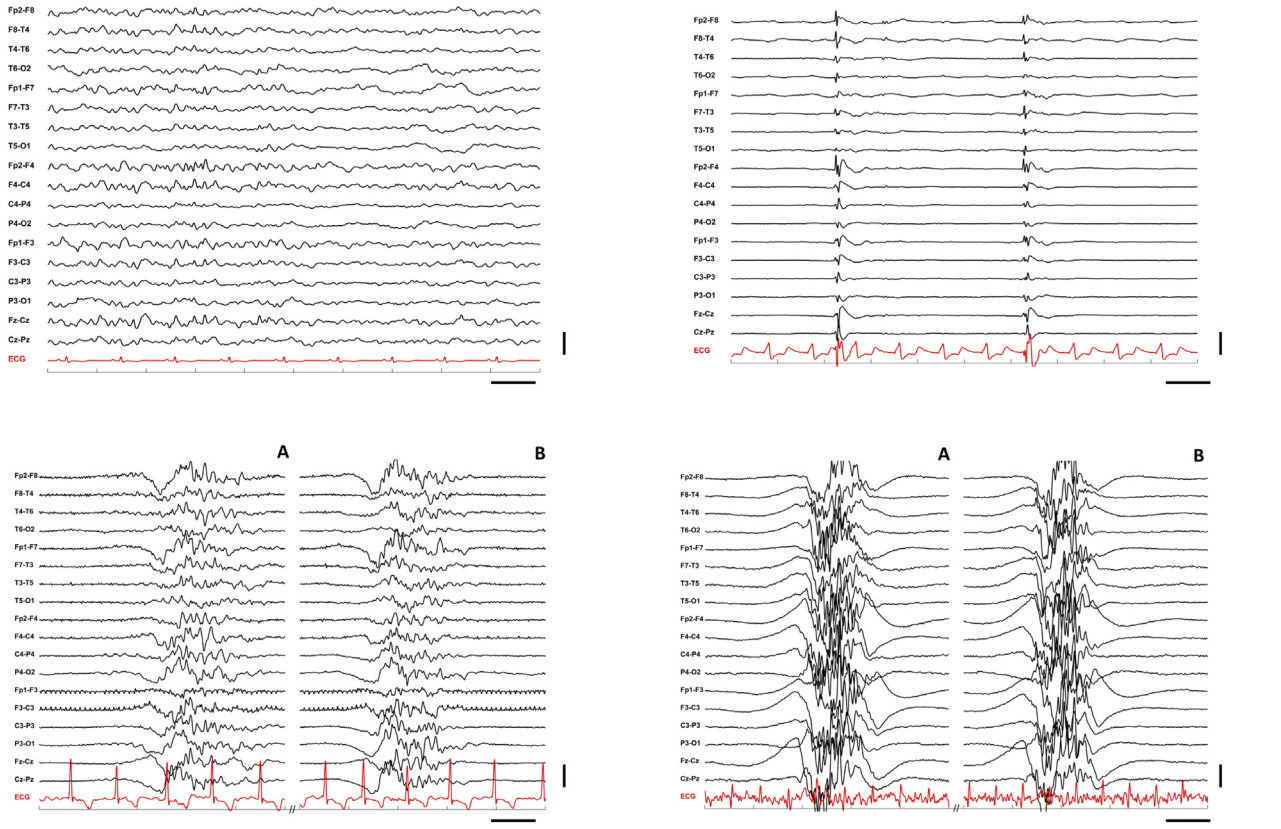

Fig. 1 – Examples of characteristic EEG patterns from four patients. Left upper panel: patient with initial good neurological recovery, showing continuous EEG 20 h after arrest. This patient died immediately after a second cardiac arrest on day 2 (case 3). Upper right: burst suppression pattern, where the bursts mainly consist of spikes (case 1). Lower left and right: burst suppression with identical bursts (cases 2 and 11, respectively.). Note the near identical waveforms of subsequent bursts for each channel comparing subpanels A and B. Time between subsequent bursts is approximately 2 s (left) and more than 50 min (right). Horizontal scale bar 1 s; vertical scale bar 50 μV.

deeper brain structures were less affected, in particular the thalamus showed no or only limited hypoxic damage. While in three of these patients, SSEP responses were preserved, prognosis was poor, in agreement with the limited sensitivity of the SSEP for poor outcome.[44,39] The pathophysiology of burst-suppression in patients with a postanoxic encephalopathy is complex, and probably includes persistent anoxic long-term potentiation of excitatory synapses.[36,6] Using these mechanisms in computational models indeed generates burst-suppression patterns similar to clinical observations.[32] Our histopathological analysis, however, did not differentiate between excitatory or inhibitory neurons to substantiate these findings.

In the two patients with a myoclonic status, postmortem histopathology showed a variable degree of Purkinje cell loss in the cerebellum and mild cortical damage with no or only mild thalamic neuronal damage. Only a few histopathological studies have been performed in patients with post-hypoxic myoclonus, showing variable degrees of neuronal loss in different structures, including cortical laminae, cerebellum, hippocampus, thalamus, and brainstem.[43,12] In an animal study of posthypoxic myoclonus, postmortem histology revealed a variable degree of neuronal injury in these brain areas, as well.[37] These observations are similar to our findings. We can only speculate how this may explain the myoclonic status, as presumably different pathophysiological mechanisms can be involved, including selective neuronal failure of inhibitory cortical neurons and involvement of the reticular thalamic nucleus.[12,41] In patients with a continuous EEG within 24 h after arrest no structural hypoxic–ischemic brain damage was present, in agreement with an intrinsic good neurological outcome.[15]

While pathological EEG patterns represent severe damage of cortical layers, it appears that hypoxic–ischemic changes limited to the cortical layers are compatible with a preserved SSEP response, if the thalamus is not, or only marginally, affected. As thalamocortical input is processed by both the deep and superficial pyramidal cells,[21,39] functional preservation of part of the cortical layers appears sufficient to record a SSEP, given a sufficiently intact thalamic relay station. In patients with bilateral absent SSEP responses, both the thalamus and the cortex were affected. These findings, although limited to a small number of patients, suggest that significant neuronal damage to the thalamo-cortical circuit is critically involved in the poor neurological outcome in patients with a bilateral absent N20 response.

Early microscopic signs of hypoxic–ischemic damage (red neurons) are first discernible histologically after survival for at least 2–6 h.[19,13,14] In tissue samples from cerebellar cortex in patients with acute or prolonged cerebral hypoxia, reduced numbers of Purkinje cells, often showing shrunken somata, were found if patients were resuscitated at least 2 h before death, using sudden death as controls.[13] In 71 patients with in hospital cardiac arrest, prolonged survival time after arrest was the only predictor of hypoxic ischemic brain injury on autopsy.[14] In rats, ischemic changes correlate with progression of survival time after arrest. For example, damaged Purkinje cells are visible approximately 5 h after the ictus, but up to 90% of the final damage becomes apparent

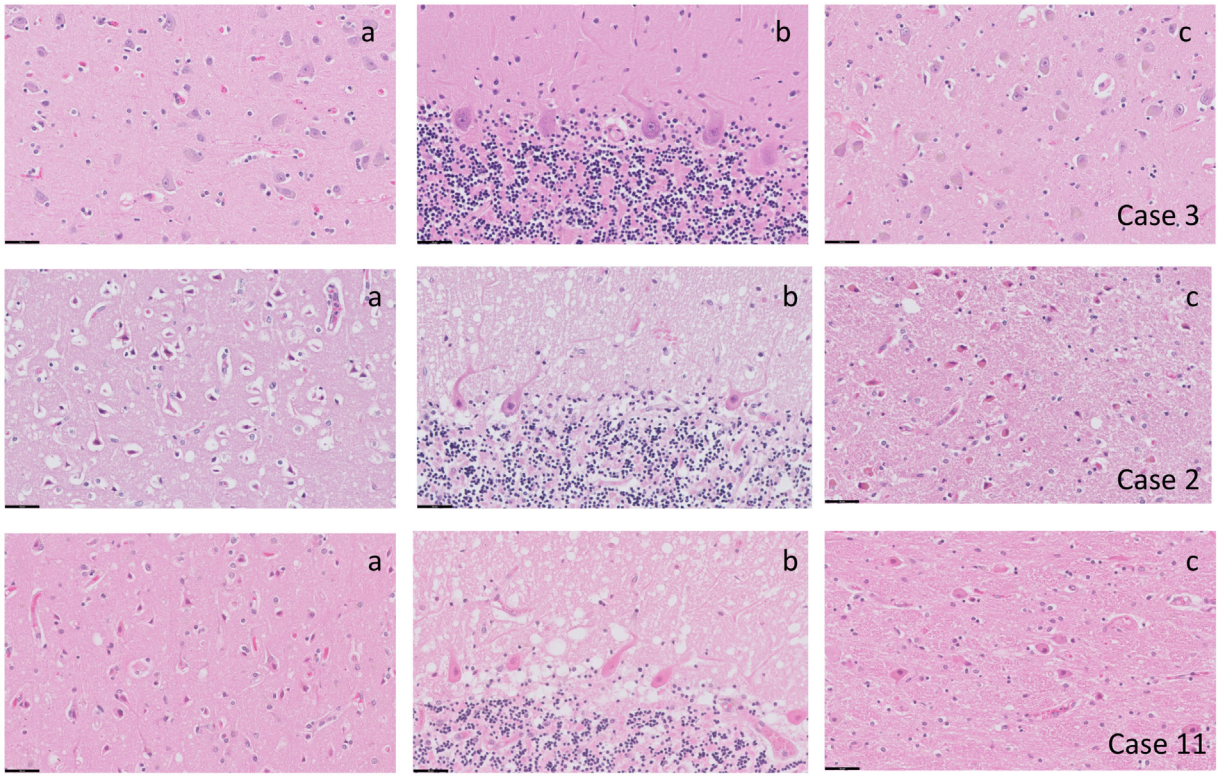

Fig. 2 – Microscopy of the frontal cortex (a), cerebellum (b) and thalamus (c) in three patients. The first row shows normal findings (case 3) in all three regions. Rows 2 and 3 show severe neuronal damage in frontal cortex, cerebellum and thalamus. Cortical neurons, Purkinje cells and thalamic neurons are shrunken, with loss of nuclear staining and the cytoplasm is more eosinophilic. In addition, vacuolization of the neuropil can be seen in the molecular layer of the cerebellum (cases 2 and 11). Scale bar = 50 μm.

Table 2 – Brain weight and distribution of hypoxic-ischemic damage, EEG pattern, SSEP and histology. n.a.: not available. Patients 3 and 10 initially recovered and died after a second arrest in the ICU. BW: brain weight; mcph: mesencephalon; hcp: hippocampus; BS: burst suppression; BSI-IB: burst suppression with identical bursts; C: continuous EEG. Grading of histology: - none, +: mild: <5%, ++: moderate: 5–50%, +++: severe: >50%. The medulla was never or only mildly (cases 2 and 5, <5%) affected.

Case	BW (g)	Cortex	hcp	Cerebellum	Thalamus	Striatum	mcph	Pons	EEG	SSEP
1	1240	+	-	+[a]	+	-	-	-	BS[c]	-
2	1325	+++	+++	+++	+++	+++	+	+++	BS-IB	-
3	1690	-	-	-	-	-	-	-	C	n.a.
4	1560	++	+++	+++	-	+	-	-	BS	+
5	1490	++	+	+++	+++	+	-	+	BS-IB	-
6	1545	+	-	+[a]	+	-	-	-	BS	+
7	1485	+++	+++	+++	+++	++	-	-	BS-IB	-[b]
8	1355	+++	+++	+++	++	+	-	+	BS-IB	-
9	1435	+	+++	+++	-	-	-	-	BS[c]-GPDs	+
10	1185	-	-	-	-	-	-	–	C	n.a.
11	1510	+++	+++	+++	+++	+++	-	-	BS-IB	-

[a] Bergmann gliosis.
[b] SSEP unilateral present.
[c] With myoclonic status.

only after more than 30 h.[5,30] In all but two of our patients, survival times varied between nearly 2–5 days, which is sufficient for microscopic signs of hypoxic damage to appear. These observations also explain why in the two patients with a second arrest (cases 3 and 10) no hypoxic–ischemic damage was observed: while neurological outcome was good, based on a continuous EEG <24 h after arrest, these patients died immediately after the second arrest, leaving no time for hypoxic–ischemic damage to develop.[11,19] Chronic lesions, characterized by the presence of laminar necrosis, usually accentuated in watershed zones, and loss of neurons with reactive gliosis, were not observed. This is not surprising as these typically develop 7–10 days after the ictus.[11]

Histological evaluation was qualitatively, focusing on the extent and distribution of neuronal damage. While morphological changes are correlated to the extent and duration of hypoxia,[29] no additional

categorization based on detailed cytological characteristics was performed. Selective vulnerability of neuronal populations is well known, hippocampus and cerebellum being most vulnerable to hypoxic ischemic incidents.[29] In our patient cohort we did not observe significant differences between cerebellum, hippocampus, cortex or deeper brain structures. This most likely results from the presence of severe brain damage in all our patients who survived longer than 2 h after arrest. The limited involvement of structural damage to the brainstem is compatible with clinical findings, showing preserved brainstem functions in most patients.[15,4] The mechanisms responsible for selective vulnerability are incompletely understood, but most likely differential failure of the sodium potassium pump[4] and the size of the extracellular space are important determinants.[3,20]

We did not perform MRI studies in our patients. The first process that fails during hypoxia is synaptic transmission that may progress to neuronal death if not restored sufficiently fast.[18,24,32,26] As this is not necessarily accompanied by cytotoxic edema, we expect that postmortem histopathology is more sensitive to detect neuronal damage than diffusion weighted MRI, as this depends on the development of cytotoxic edema.[2,26,22]

Limitations of our study include the small number of patients and the qualitative assessment of histopathological changes. Despite these shortcomings, we show that the severity of EEG abnormalities correlates with the extent and distribution of hypoxic–ischemic brain damage, in agreement with previous reported associations between early EEG and neurological outcome.[15,34] In particular, in patients with burst-suppression with identical bursts, extensive hypoxic–ischemic damage is present in the cerebellum, cortical layers and thalamus. All patients with absent SSEP responses had thalamic damage.

Author contributions

MvP, MCT-C and JH conceived the idea for this study. CJ and RK performed postmortem analysis. EEG interpretation was performed by MvP or MCT-C. Writing of first draft: MvP. AB and FB were responsible for treating the patients in the ICU and obtaining consent from the family for the postmortem analysis. All authors commented on the first draft and approved the final version.

Conflict of interest

Michel JAM van Putten is a co-founder and medical advisor of Clinical Science Systems, a manufacturer of software for EEG monitoring

The other authors have no conflict of interest to declare.

Acknowledgements

The lab technicians are acknowledged for assisting in EEG recordings.

REFERENCES

1. Bandera E, Botteri M, Minelli C, Sutton A, Abrams KR, Latronico N. Cerebral blood flow threshold of ischemic penumbra and infarct core in acute ischemic stroke: a systematic review. Stroke 2006;37:1334–9.
2. Bolay H, Gürsoy-Özdemir Y, Sara Y, Onur R, Can A, Dalkara T. Persistent defect in transmitter release and synapsin phosphorylation in cerebral cortex after transient moderate ischemic injury. Stroke 2002;33:1369–75.
3. Brisson CD, Andrew RD. A neuronal population in hypothalamus that dramatically resists acute ischemic injury compared to neocortex. J Neurophysiol 2012;108:419–30.
4. Brisson CD, Hsieh YT, Kim D, Jin AY, Andrew RD. Brainstem neurons survive the identical ischemic stress that kills higher neurons: insight to the persistent vegetative state. PLOS ONE 20149:.
5. Busl KM, Greer DM. Hypoxic–ischemic brain injury: pathophysiology, neuropathology and mechanisms. NeuroRehabilitation 2010;26:5–13.
6. Calabresi P, Centonze D, Pisani A, Cupini L, Bernardi G. Synaptic plasticity in the ischaemic brain. Lancet Neurol 2003;2:622–9.
7. Cloostermans MC, van Meulen FB, Eertman CJ, Hom HW, van Putten MJAM. Continuous electroencephalography monitoring for early prediction of neurological outcome in postanoxic patients after cardiac arrest. Crit Care Med 2012;40:1.
8. de Oliveira JL, Crispin PdTB, Duarte ECW, et al. Histopathology of motor cortex in an experimental focal ischemic stroke in mouse model. J Chem Neuroanat 2014;57–58:1–9.
9. Dijkstra K, Hofmeijer J, van Gils S, van Putten M. A biophysical model for cytotoxic cell swelling. J Neurosci 2016;36:11881–90.
10. Fedorovich S, Hofmeijer J, van Putten M, le Feber J. Reduced synaptic vesicle recycling during hypoxia in cultured cortical neurons. Front Cell Neurosci 2017;11:1–8.
11. Garcia JH, Liu K-F, Ho K-L. Neuronal necrosis after middle cerebral artery occlusion in Wistar rats progresses at different time intervals in the caudoputamen and the cortex. Stroke 1995;26:636–43.
12. Gupta HV, Caviness JN. Post-hypoxic myoclonus: current concepts, neurophysiology, and treatment. Tremor Other Hyperkinetic Mov (New York, NY) 2016;6:409.
13. Hausmann R, Seidl S, Betz P. Hypoxic changes in Purkinje cells of the human cerebellum. Int J Leg Med 2007;121:175–83.
14. Hinduja A, Gupta H, Yang JD, Onteddu S. Hypoxic ischemic brain injury following in hospital cardiac arrest– lessons from autopsy. J Forensic Leg Med 2014;23:84–6.
15. Hofmeijer J, Beernink T, Bosch F, Beishuizen A, Tjepkema-Cloostermans M, van Putten M. Early EEG contributes to multimodal outcome prediction of postanoxic coma. Neurology 2015;85:1–7.
16. Hofmeijer J, Mulder ATB, Farinha AC, van Putten MJAM, le Feber J. Mild hypoxia affects synaptic connectivity in cultured neuronal networks. Brain Res 2014;1557:180–9.
17. Hofmeijer J, Tjepkema-Cloostermans MC, van Putten MJaM. Burst-suppression with identical bursts: a distinct EEG pattern with poor outcome in postanoxic coma. Clin Neurophysiol 2013.
18. Hofmeijer J, Van Putten M. Ischemic cerebral damage: an appraisal of synaptic failure. Stroke 2012;43:607–15.
19. Horn M, Schlote W. Delayed neuronal death and delayed neuronal recovery in the human brain following global ischemia. Acta Neuropathol 1992;85:79–87.
20. Hübel N, Andrew RD, Ullah G. Large extracellular space leads to neuronal susceptibility to ischemic injury in a Na^+/K^+ pumps-dependent manner. J Comput Neurosci 2016;40:177–92.
21. Ikeda H, Wang Y, Okada YC. Origins of the somatic N20 and high-frequency oscillations evoked by trigeminal stimulation in the piglets. Clin Neurophysiol 2005;116:827–41.
22. Keijzer H, Hoedemaekers C, Meijer F, Tonino B, Klijn C, Hofmeijer J. Brain imaging in comatose survivors of cardiac arrest: pathophysiological correlates and prognostic properties. Resuscitation 2018;133:124–36.
23. Khazipov R, Congar P, Khazipov R, Congar P, Ben-Ari Y. interneurons: comparison of effects of anoxia on excitatory and inhibitory postsynaptic currents hippocampal CA1 lacunosum–moleculare interneurons: comparison of effects of anoxia on excitatory and inhibitory postsynaptic currents. J Neurophysiol 1995;74:2138–49.
24. Le Feber J, Pavlidou S, Erkamp N, Van Putten M, Hofmeijer J. Progression of neuronal damage in an in vitro model of the ischemic penumbra. PLOS ONE 201611:.

25. Makin SDJ, Doubal FN, Dennis MS, Wardlaw JM. Clinically confirmed stroke with negative diffusion-weighted imaging magnetic resonance imaging: longitudinal study of clinical outcomes, stroke recurrence, and systematic review. Stroke 2015;46:3142–8.
26. Makin SDJ, Doubal FN, Dennis MS, Wardlaw JM. Clinically confirmed stroke with negative diffusion-weighted imaging magnetic resonance imaging: longitudinal study of clinical outcomes, stroke recurrence, and systematic review. Stroke 2015;46:3142–8.
27. Miyake S, Tanaka M, Matsui K, et al. [Mortality patterns of children with epilepsies in a children's medical center]. No To Hattatsu 1991;23:329–35.
28. Mlynash M, Campbell DM, Leproust EM, et al. Temporal and spatial profile of brain diffusion-weighted MRI after cardiac arrest. Stroke 2010;41:1665–72.
29. Pae EK, Chien P, Harper RM. Intermittent hypoxia damages cerebellar cortex and deep nuclei. Neurosci Lett 2005;375:123–8.
30. Reeves SR, Gozal E, Guo SZ, et al. Effect of long-term intermittent and sustained hypoxia on hypoxic ventilatory and metabolic responses in the adult rat. J Appl Physiol (Bethesda, Md.: 1985) 2003;95:1767–74.
31. Rossetti AO, Quiroga DFT, Juan E, et al. Electroencephalography predicts poor and good outcomes after cardiac arrest: a two-center study. Crit Care Med 2017;1–9.
32. Ruijter B, Hofmeijer J, Meijer H, van Putten M. Synaptic damage underlies EEG abnormalities in postanoxic encephalopathy: a computational study. Clin Neurophysiol 2017;128:1682–95.
33. Rungta RL, Choi HB, Tyson JR, et al. The cellular mechanisms of neuronal swelling underlying cytotoxic edema. Cell 2015;161:610–21.
34. Sondag L, Ruijter BJ, Tjepkema-Cloostermans MC, et al. Early EEG for outcome prediction of postanoxic coma: prospective cohort study with cost-minimization analysis. Crit Care 2017;21:111.
35. Spalletti M, Carrai R, Scarpino M, et al. Single electroencephalographic patterns as specific and time-dependent indicators of good and poor outcome after cardiac arrest. Clin Neurophysiol 2016;127:2610–7.
36. Szatkowski M, Attwell D. Triggering and execution of neuronal death in brain ischaemia: two phases of glutamate release by different mechanisms. Trends Neurosci 1994;17:359–65.
37. Tai KK, Bhidayasiri R, Truong DD. Post-hypoxic animal model of myoclonus. Parkinsonism Relat Disord 2007;13:377–81.
38. Urban NN, Barrionuevo G. Induction of Hebbian and non-Hebbian mossy fiber long-term potentiation by distinct patterns of high-frequency stimulation. J Neurosci 1996;16:4293–9.
39. van Putten M. The N20 in post-anoxic coma: are you listening? Clin Neurophysiol 2012;123:1460–4.
40. Van Putten M, Hofmeijer J. EEG monitoring in cerebral ischemia: basic concepts and clinical applications. J Clin Neurophysiol 201633:.
41. van Zijl JC, Beudel M, vd Hoeven HJ, Lange F, Tijssen MAJ, Elting JWJ. Electroencephalographic findings in posthypoxic myoclonus. J Intensive Care Med 2016;31:270–5.
42. Westhall E, Rossetti AO, Van Rootselaar AF, et al. Standardized EEG interpretation accurately predicts prognosis after cardiac arrest. Neurology 2016;86:1482–90.
43. Young GB, Gilbert JJ, Zochodne DW. The significance of myoclonic status epilepticus in postanoxic coma. Neurology 1990;40:1843–8.
44. Zandbergen EGJ, Koelman JHTM, de Haan RJ, Hijdra A, Group P.R.O.P.A.C.-S. SSEPs and prognosis in postanoxic coma: only short or also long latency responses? Neurology 2006;67:583–6.